Determination of Aerodynamic Vibration Excitation on UAV Rotors Using CFD Simulations

Shantesh Rai

CMS-CE

D.o.B -▬▬▬▬▬

Matriculation Number-▬▬▬▬

Research Project Report

Supervisor

Dipl.-Ing. David Bernstein

Supervising University Teacher

Prof. Dr.-Ing. Michael Beitelschmidt

Table of Contents

Table of Figures

Index of Tables

TASK DESCRIPTION FOR THE RESEARCH PROJECT

Degree Course: **Computational Modeling and Simulation (CMS)**

Module: **CMS-PROJ Research Project**

Student name: **Rai, Shantesh**

Matriculation number: ████████

Topic title: Determination of aerodynamic vibration excitation on UAV rotors using CFD-Simulations

Motivation

Induced by the thrust units, UAVs are exposed to a high vibration level. For aerial manipulation tasks, UAVs are equipped with various sensors that are sensitive to vibrations. Vibration damping at the sensor mounting is often used to reduce the vibration level. However, it would be better to reduce the induced vibration excitation at the thrust unit or its mounting. For this, the main sources of vibration excitation for each direction have to be identified. In the direction of thrust force, vibration excitation can result from aerodynamic turbulences. To investigate the influence of this effect, numerical flow simulations are to be used in the student project.

Objective

Rotor flow simulation models are existing from previous student projects with thrust and torque errors between 1 – 5 % compared to experimental data. Using ANSYS FLUENT, these models can be further developed to investigate the vibration excitation of the propellers. If necessary, also new modelling approaches can be tested and compared with the existing ones. The time curves of thrust and torque are to be analysed regarding vibration level and order using FFT analysis.

Tasks

- Familiarization with rotor flow simulation using the CFD Software ANSYS FLUENT based on previous student thesis

- Literature study on vibration excitation by UAV rotors and state of the art in rotor flow simulation

- Simulation of the rotor flow of a single rotor, analysis of rotor thrust and torque and validation using measurements

- Optimization of the rotor flow simulation for vibration excitation analysis

- FFT analysis of the time curves of rotor thrust and torque

- Documentation and discussion of the results

Examiner: Prof. Dr.-Ing. Michael Beitelschmidt, TU Dresden

Supervisor: Dipl.-Ing. David Bernstein, TU Dresden

Starting date: 01.10.2021

End date: 25.02.2022

The guidelines issued by the degree course for the preparation of the thesis and the examination regulations must be observed.

A digital appendix to the work must be submitted (data CD, etc.). This must include all models, calculations and simulation results documented in the report with the necessary input data and parameters as well as the scripts and programs used to create the models. If necessary, a meeting with the supervisor must be arranged before the presentation, in which the data appendix is showed and explained.

The module examination consists of completing a project of 450 hours, and a 30 minutes presentation in English.

_____   _____

Dipl.-Ing.
David Bernstein   Shantesh Rai
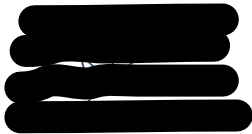
Supervisor   Student

DECLARATION OF INDEPENDENT-WORK

I hereby assure, that I have written my research project report *Determination of aerodynamic vibration excitation on UAV rotors using CFD-Simulations* independently, without the impermissible help of third parties and without the use of any aids other than those specified. The thoughts taken directly or indirectly from external sources are marked as such and the sources are indicated. I have not yet submitted the work in this or a similar form or in part as part of another examination.

Dresden, 25 February 2022

Shantesh Rai

Abstract

UAVs are mounted with a number of sensors to assist flight and manoeuvrability. The data from these sensors are vulnerable to noises that are introduced due to the vibrations in the drone. These vibrations also pose challenge to the structural integrity of the drone body. Various sources of these vibrations have been identified and studied. One of the source that is taken up in this research project is the aerodynamic turbulence, that occur in the fluid flow around the propeller. CFD models were developed to get the thrust and moment curves. Five different models were made, compared and validated against the experimental data in a bid to find the optimum model. Vibration analysis was carried by applying FFT transformation on the output thrust and moment curves. The transformed curves show wave amplitudes at expected frequency values.

1. Introduction

Since the last decade, the application of small Unmanned Aerial Vehicles (UAV), popularly known as drones, has seen a significant growth in many fields viz. photography, agriculture, surveillance, logistics and so on. The spectrum of their application field is continuously expanding. Ergo, a lot of study is being conducted to optimize their performance and control. UAV stabilization and navigation require flight data which is collected by various onboard sensors like gyroscope, accelerometer, GPS, to name a few.

Accurate noise-free sensor data is paramount for precise and safe manoeuvre. Induced by the thrust units, UAVs are exposed to a high vibration level. Vibrations form the major proportion of the noise in the data. Not only the sensor data, but also the structural integrity of the drone body and propeller is vulnerable due to vibrations.

Vibration damping at the sensor mounting is often used to reduce the vibration level. However, it would be better to reduce the induced vibration excitation at the thrust unit or its mounting. For this, the main sources of vibration excitation for each direction have to be identified. In the direction of the thrust force, vibration excitation can result from aerodynamic turbulences. To investigate the influence of this effect, numerical flow simulations were used within this project.

The rest of the report is structured in the following manner. Section 2 establishes the objective of the research project. Section 3 lays the basic theoretical background of CFD simulations and propeller flows. Section 4 is dedicated to the summary of literature survey that was done to study and find the state-of-the-art methods applied for propeller flow simulation. The vibration in UAVs was also studied during the survey. Section 5 explains the methodology used to develop the CFD models. Section 6 presents the outputs and discussions. Finally, section 7 concludes the report.

2. Objective

Rotor flow simulation models are existing from previous student projects with thrust and moment errors between 1 – 5 % compared to experimental data. Using ANSYS FLUENT, these models can be further developed to investigate the vibration excitation of the propellers. If necessary, also new modelling approaches can be tested and compared with the existing ones. The time curves of thrust and moment are to be analysed regarding vibration level and order using FFT analysis.

The pedagogy for this research project can be streamlined as follows:-

- Familiarization with rotor flow simulation using the CFD Software ANSYS FLUENT based on previous student thesis
- Literature study on vibration excitation by UAV rotors and state of the art in rotor flow simulation
- Simulation of the rotor flow of a single rotor, analysis of rotor thrust and moment and validation using measurements
- Optimization of the rotor flow simulation for vibration excitation analysis
- FFT analysis of the time curves of rotor thrust and moment
- Documentation and discussion of the results

3. Theoretical Background

3.1 Propeller Geometry and Aerodynamics[1]

A propeller is a rotating device that consists of two or more blades attached to a central hub at a fixed pitch in a helical pattern. Its working principle is based on *Archimedes' screw*. By rotating in a fluid, it converts input rotational power to axial thrust. The twisted blade design of an aircraft propeller (or airscrew) was pioneered by *Wright Brothers*, who realised that an air propeller blade was essentially a wing. The twist was necessary to ensure the same angle of attack along wing-span. Conversely, one can view a propeller blade as composed of many aerofoil sections having different pitch angles. It is the pressure differential between the upper and lower face of these aerofoils which result in the total thrust force, when the propeller rotates.
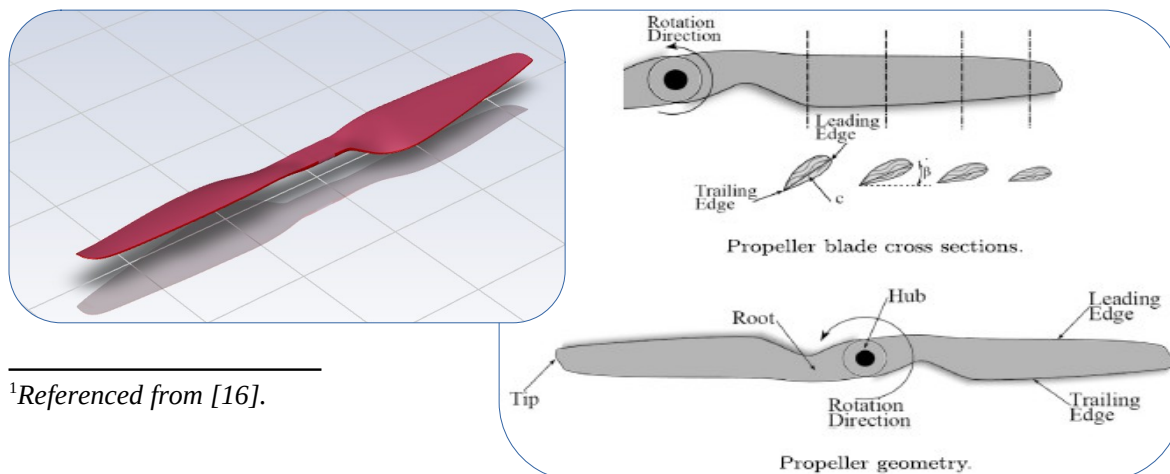

_____

[1]*Referenced from [16].*

Figure 1: Characteristics of a Propeller. Adopted from [1], [13]

Figure [1] shows the geometric attributes of a propeller. The *leading edge* is the first point of contact between the blade and fluid. The *trailing edge* is the last point of contact. *D* is the diameter of the propeller and *c* is the distance between the leading and trailing edges, called as the *chord length*. *β* is the pitch angle that each foil section makes with the rotating plane. Moreover, for this project *n* is the number of rotations per minute, *T* is the thrust produced along axis of rotation and *M* is the moment experienced by the blade due to airflow. As mentioned in (Vargas 2021), following are some characteristic coefficients which are used to analyse the propeller performance:

$$K_T = \frac{T}{\rho n^2 D^4} \quad K_p = \frac{P}{\rho n^3 D^5} \quad J = \frac{V}{n D} \quad \eta = J \frac{K_T}{K_P}$$

Here, ρ, V, P are the air density, advance velocity and power, respectively. K_T and K_P are dimensionless coefficients; J is the advance ratio; and η is the propeller efficiency.

3.2 CFD Simulation[2]

Every CFD numerical simulation has a general logic of working. There are four fundamental equations that are applied for every problem viz. the continuity equation and three momentum equations for each direction. Apart from these equations, some more equations can be solved based on the problem being solved. All these equations are partial differential equations. Since the equations cannot be solved for a continuous domain due to the computational and memory limitations, therefore the whole domain is broken down into small volumes (cells). These equations are then formulated for these finite number of volume cells and this process is termed as discretization of the equations. In the case of ANSYS FLUENT solver, all the flow variables that result during the iterative solution of the equations are stored at the cell centre. In order to get an accurate solution, the size of the cells should be small enough to properly resolve the various scales of flow parameters, like eddies in case of turbulent flows. Once the cell-centre values are calculated, it is then interpolated to the cell-face in order to calculate the convection of the flow. The final cell-centre values are then used to plot the contour, vectors or even calculate variables and functions of these variables in CFD-Post to visualize and analyse the generated solution. The workflow of a typical CFD analysis can be summarized as:

- Modelling the geometry/flow-domain
- Generating the mesh
- Setting up the solver
- Running the simulation
- Post-processing and analysing

3.2.1 Boundary Layer Theory[3]

Due to the inter-molecular forces of attraction, viscous forces arise in fluid flows. When a fluid flows near a surface, the molecules in the immediate vicinity of the surface comes to rest with

---

[2]*For complete CFD theory and equation derivations refer (Tuncer Cebeci 2005).*

[3]*This section is a summarized theory. For full-text and comprehensive reading refer .(Çengel 2010)*

respect to the surface. This is called the *no-slip condition*. The fluid layers above, are also slowed down. However, this wall effect wears-off for each successive layer until the fluid velocity becomes equal to free-stream velocity, thereby creating a velocity gradient in the wall-perpendicular direction. This region of fluid flow near a wall is called the *boundary layer*.

Near the leading edge, the boundary layer is thin and entirely *laminar*. As the fluid moves ahead along the surface, the boundary layer thickness increases and the laminar flow becomes unstable. Ultimately, these irregularities makes the flow *turbulent* and the boundary layer thickens rapidly. This change from laminar to turbulent flow takes place over a short length, called as *transition region*.

The turbulent flow is characterized by high velocity fluctuations and eddies. Eddies of arbitrary size are formed and broken, moves randomly between the fluid layers and coalesce/degrades into different length-scales. All of these lead to transfer of energy, particles and momentum between the layers, resulting in thicker and homogeneous boundary layer. Experimental results show that within the turbulent boundary layer, there are three distinct regions:-

1. Viscous/laminar sub-layer
2. Buffer layer
3. Fully-Turbulent layer
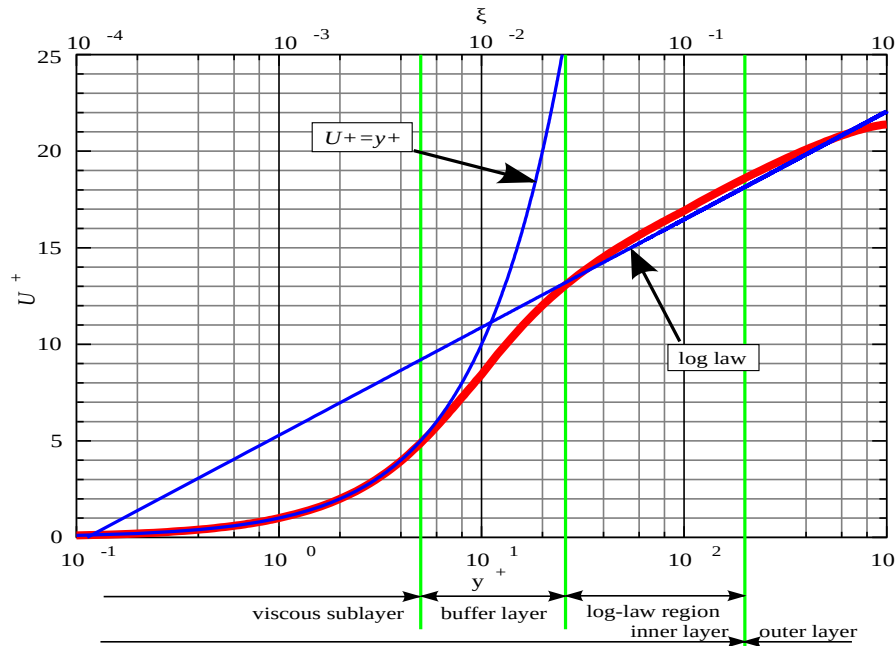
Figure 2: Law of the Wall. Obtained from [12]

The presence of the viscous sub-layer can be explained by the presence of wall. Not only the wall viscous effects are dominant than the inertial force of the flow, the formation and existence of eddies is obstructed by the presence of the wall. While the velocity profile for the sub-layer is almost linear, the average-velocity profile of the turbulent layer is a logarithmic function of the distance of a point from the wall and is known as *logarithmic law of the wall* or simply, *law of the wall*. *Figure [2]* shows the graph of velocity profile function in different regions of the

turbulent flow. Here, U^+ is the dimensionless velocity and y^+ is the dimensionless distance from the wall. Neither the linear law nor the log-law of the wall is applicable in the buffer layer.

In the context of CFD simulations, near-wall or boundary layer modelling have significant effect on the fidelity of numerical solutions, since this region have large gradients and pronounced transport of scalar quantities. There are two approaches to model boundary layer, namely *wall functions* approach and *near-wall model* approach. While semi-empirical formulas are used to model the viscous sublayer and buffer layer in wall function approach, a very fine mesh is used to actually resolve both regions in near-wall model approach. The former is useful for most high Reynolds number flows since it is robust, computationally economic and fairly accurate, while the latter is used for flows where low Reynolds number effect come into play as is the case for this project. Since there is no accurate profile function for buffer layer, therefore it is imperative to keep $y^+<5$. As a research standard, $y^+<1$ was targeted and achieved for this project as shown in the *figure [3]*.
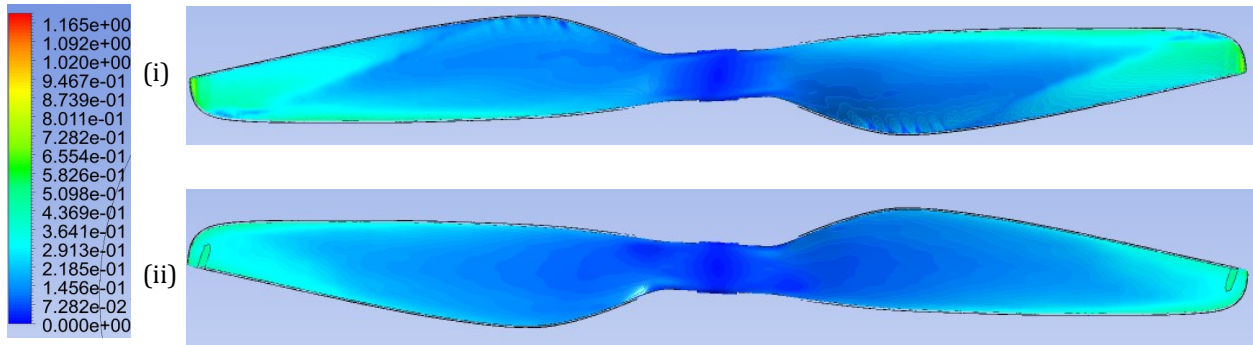

Figure 3: y^+ Contours on (i) Upper Face of Propeller , (ii) Lower Face of Propeller

3.2.2 Turbulence Modelling[4]

Turbulent flows are characterized by random eddies and fluctuations of velocity fields and other transported scalar quantities. These fluctuations can have a very small length-scale and high frequency. It is practically infeasible to numerically simulate time-dependent high Reynolds-number flows for complex geometries with all fluctuation scales due to high computational costs. It is due to this reason, that a *direct numerical simulation (DNS)* of Navier-Stokes equations, which is a technique where eddies are resolved in the entire range of spatial and temporal scales, is not employed in real engineering world. Alternatively, the governing equations are modified by using mean quantities or time-averaging or filtering out small-scales. These modified equations contains additional unknowns but are computationally economic to solve. In order to determine these new unknowns in terms of the known variables, turbulence modelling is done, which introduces additional scalar transport equations.

Two of the most prevalent modification methods are: *Reynolds-averaging* and LES (*Large Eddy Simulation*) method. In the LES approach, a mathematical filter is used over Navier-Stokes Equations to exclusively resolve eddies till a certain length-scale. All the remaining smaller eddies are then modelled in the equation. Doing this reduces the error due to turbulence

---

[4]*Inc. ANSYS. Ansys online help, October 2021.*

modelling, since more eddies are resolved rather than modelled. As a ramification, the computational costs are still relatively high which makes this approach impractical in the industry. In the Reynolds-averaging approach, the transport flow quantity is decomposed as a sum of mean value and fluctuation value, and then the equations are expressed in terms of mean value. This results in an extra unknown term in the equations, composed of fluctuation values, called as *Reynolds stress*. This stress term represents the cumulative effect of eddies of all scales, effectively modelling all the eddies in the flow. These modified equations are called *Reynolds-averaged Navier-Stokes (RANS)* equations. The RANS based models require less computational effort and resource, thereby making it viable for engineering applications.

The turbulence modelling using Reynolds-averaging approach boils down to modelling the Reynolds stress term in RANS equations. There are two family of models which achieve this, namely, *Boussinesq Approach Models* and *Reynolds Stress Transport Models (RSM)*. The RSM approach is more comprehensive, involves less assumptions and employs five to seven additional equations, making it more expensive to solve. Hence, it is only used for highly swirling flows where eddies are highly anisotropic. On the other hand, Boussinesq approach assumes eddies to be isotropic and having dynamics analogous to Brownian motion to model the Reynolds stress in terms of mean values and an additional factor called *turbulent viscosity, μ_t*. This makes Boussinesq approach models relatively low-cost and highly practical.

The Boussinesq family of models accommodates the most popular RANS models viz. $k\epsilon$ family, $k\omega$ family and Spalart-Allmaras model. These models just differ in the way they determine μ_t and the number of additional scalar transport equations used. The earliest model was $k\epsilon$, which used *turbulent kinetic energy k* and *turbulence dissipation rate ϵ* to calculate μ_t. But it performed badly in the near-wall region. Then came $k\omega$ model which replaced ϵ with *specific dissipation rate ω* as a remedy. While its superiority was palpable in near-wall region, it was sensitive to inlet condition and free-stream flow. A new model $k\omega$-*SST* ensued, which used a transformation factor based on distance from wall, such that the model would act as $k\omega$ in the near-wall region and transform into $k\epsilon$ in the far free-stream region. All these models employs two additional scalar transport equations for either k and ϵ or k and ω. However, these models were inherently designed for high Reynolds-number flows and therefore, produce inaccuracies for low *Reynolds-number* turbulent flows. To address this issue, the $k\omega$-*SST* model was appended with two more additional scalar equations to accommodate the laminar and transition regions prior to the fully turbulent region. This 4-equation model is called *Transition-SST* model and it estimates the flow transition and its location with better accuracy.

3.3 Propeller Flow Simulation Techniques[5]

For the aerodynamic study of propeller, the fluid flow around the moving propeller is of interest rather than the propeller motion. When viewed from the inertial reference frame, the moving propeller render the problem unsteady. Therefore, it is advantageous to solve the equations in the propeller's frame of reference, since the flow can be modelled as a steady-state problem with respect to the propeller frame. ANSYS FLUENT provides moving reference frame modelling which enables transforming the equations in propeller's rotating frame. The original equations of

---

[5]*Inc. ANSYS. Ansys online help, October 2021.*

motion are modified to account for the rotational effects, namely *Coriolis effect* and *Centrifugal force,* and this modification is manifested in the form of source terms in the original equations. However, applying these modifications on the entire domain will produce artefacts. Hence, the domain is divided into a rotating zone (disk) and a stationary zone. The rotating zone contains the propeller and the modified equations are solved in this zone only, while solving the normal equations for the stationary zone. Both the zones are bounded by their defined interface and are connected to each other at the interfaces. Based on the type of interface interaction, two popular types of modelling are possible for propeller simulation: *Multiple Reference Frame (MRF)* and *Sliding Mesh*.

MRF method, also known as *Frozen rotor method*, is a steady-state approximation where there is no relative motion between the two zones throughout the simulation. The equation transformations are made as soon as the frame changes. Local reference frame transformations are performed at the interface between cell zones, to enable the variables of one zone to be used to determine the fluxes at the adjacent zone boundary. However, the transient effects and flow mixing is not modelled at the interface which results in unreal results. Also, the results are not time-accurate rather time-averaged.

Sliding Mesh technique is an inherent transient method, since the rotating zone actually rotates with respect to the stationary zone and the flow variables are interpolated across the interface at every timestep. It produces time-accurate solution for unsteady flow and due to this transient behaviour it is computationally expensive. Since this project is about aerodynamic vibration analysis, therefore this is the only applicable method to produce time-accurate thrust and moment curves.

4. Literature survey

The study and identification of various vibration source is being done by researchers and industry, to either exploit or minimize or eliminate their effects. The motor-propeller units were identified in (Verbeke 2016), (Kuantama 2021) and (Mizui 2012) as the main source of axial and radial vibrations. The experimental data in (Verbeke 2016) shows an almost quadratic relation between vibration force amplitude and rotation frequency which signalled propeller imbalances. The obtained vibration patterns were used to develop a structural finite-element model of the drone and conduct design simulations. Analyses in (Kuantama 2021) establishes a relation between propeller's rotational speed and vibration as well as compare the effect of balanced and unbalanced propeller on quadcopter's thrust and performance. The vibrations due to propeller imbalance, as found by the authors in (Mizui 2012), when became resonant with the natural frequency of the drone-arm and other parts, causes distortion in sensor data which is detrimental to flight-stability and control. The correlation between propeller thrust, propeller rotation speed and natural frequency of the designed part was elucidated, so as to eliminate resonance. A different source of vibration was identified in (Radkowski 2015) which arises due to drone rotation around pitch and/or roll axis. These vibrations are more perceivable than the ones caused by unbalanced motor/propeller. The underlying physics and mathematical model were explained

and simulations were conducted to explore the possibilities to abate or to eliminate such vibrations.

This research project investigates another source of vibration viz. aerodynamic turbulences. Hence, the aerodynamic study of propeller is going to be the focal point of this project. (Vargas 2021) emphasized on the difficulty to determine the aerodynamic performance of UAV propellers due to their small-size and low values of operating conditions. These propellers generally operate in the low Reynolds number regime and therefore the complexities of the transition region comes into play. A comparative study was conducted between a low-fidelity method, blade element momentum theory (BEMT), and a high-fidelity method, 3D computational fluid dynamics (CFD), using wind tunnel test data as benchmark. It was concluded that while BEMT was suited for low advance ratio conditions due to its low computational cost, it's still an inferior tool since it was unable to account for 3D effects and turbulence for higher advance ratio flow conditions. On the contrary, CFD's high computational cost was amortized by its capability for 3D simulation, producing physically more germane and accurate results.

When it comes to CFD analysis of a propeller, there are two approaches that are most widely used, namely frozen rotor or multiple reference frame(MRF) approach and sliding mesh method. Both these methods were employed and compared in (Vargas 2021). Results showed that the frozen rotor approach suffered numerical diffusion but took significantly less computational resource and time. On the contrary, sliding mesh method produced less deviation from wind tunnel data but took higher computational resource and effort. It was summarized that while frozen motor approach can be used for quick simulative study, sliding mesh method should be considered for comprehensive study in real-world application. In (Krishnamurthy 2020) where flow field around marine propeller was modelled, it was pointed out that MRF approach fails to accurately determine the amplitude of the fluctuating forces and is sensitive to the position of the downstream interface between the rotatory and stationary zones. For the characterisation of flow around a quadcopter propeller and overall thrust performance of the drone, both these methods were used and compared in (Paz 2021). The results for the ground effect study for single propeller revealed both methods as qualitatively equivalent. A difference of 11% was found in the quantitative study between the methods. Despite of having lower accuracy, MRF due to its significantly lower computational requirements, was deemed a better option for preliminary test studies. The results and conclusion were similar for the simulation of entire quadcopter. In (Fu 2012), MRF method was employed to simulate the slipstream flow of a propeller and it gave good agreement with the experimental data. It was then used to investigate the aerodynamic interference between the wing of an UAV and its propeller. MRF was put to use in (LaCroix and Máca) where a validation study was conducted for a proprietary CFD solver and meshing software against the benchmark experimental data of a marine propeller.

Investigative studies of transition flow over a model propeller blade were presented in (Yao 2017). Experiments showed that the transition point was affected by inflow Reynolds number, turbulence intensity and the pressure gradient over the blade surface. A mathematical model was also derived to estimate the transition location on the propeller blade. Furthermore, various turbulence models were also tested and it was observed that both *kω-SST* and *realizable-kε* were

unable to accurately predict the transition. An extended version of *kω-SST* model called *γ-Re* transition model (nowadays *Transition-SST* model) gave the accurate results for transition location.

5. Methodology

The flow simulations for this research project were carried out on the commercial CFD software ANSYS FLUENT 2020R2. The propeller CAD model was taken from previous diploma project (Korfmann 2020). Required CAD modification and creation of the fluid domain was done in ANSYS DesignModeler. This was followed by meshing for which ANSYS Mesh as well as ANSYS FLUENT were used. The stimulation jobs were run on TU Dresden's HPC cluster *'Taurus'*. Following sections describe the modelling steps, namely domain modelling, meshing and model case setup.
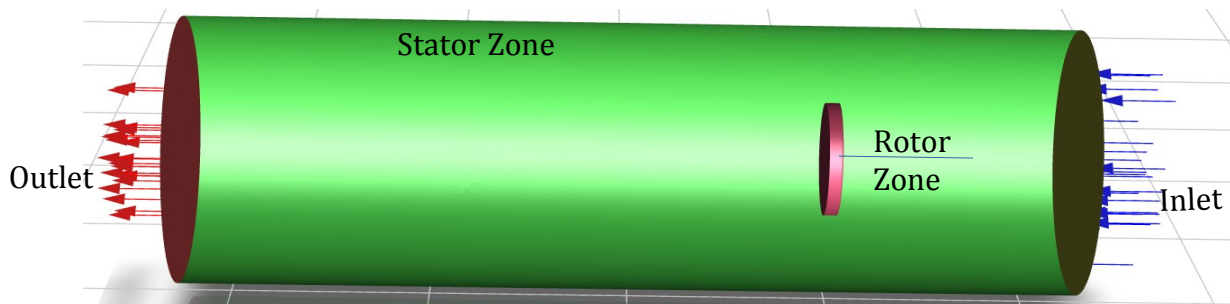
5.1 Domain Modelling

Figure 4: Flow Domain

Figure [4] shows the computational domain. The entire domain is divided in two zones: Rotor and Stator. The rotor is the inner cylinder which contains the propeller. The stator is the outer big cylinder having an inlet, an outlet and a wall. An interface is defined between the rotor zone and the stator zone. The diameter D of the propeller is 380 mm. The propeller and zone axes are aligned to y-direction and the origin of the coordinate systems lie at the centroid of the rotor zone. The propeller rotates in counter-clockwise direction and the thrust is generated in the y-direction. The zone dimensions and boundary conditions are as follows:-

- Rotor Zone: cylinder with diameter of 1.1D (418 mm) and height of 0.108D (41 mm).
- Stator Zone: cylinder with diameter of 2.6D (988 mm) and height of 7.207D (2739 mm).
- Inlet Face: a pressure inlet
- Outlet Face: a pressure outlet
- External Curve Wall: symmetry boundary condition
- Propeller Surface Wall: no-slip condition
- Interface Between Rotor and Stator: sliding mesh interface

As a good CFD practice, the topography of the CAD model was improved to remove small edges and slivers to simplify the domain for meshing.

5.2 Meshing and mesh convergence study

Once the domain is ready, it is moved to the mesher application. It is a well-known fact that hexahedral mesh is the most efficient (volumetric packing) and robust mesh, and takes least time and effort to give the most accurate results. But with a complex geometry like that of a propeller, it is not possible to generate a hex mesh in the entire domain. Therefore, the next best option as concluded in (Korfmann 2020), is using polyhedral mesh. Hence, the stator is meshed using hexahedral element type in ANSYS Mesh while the rotor zone (*Figure [6]*) is separately meshed with polyhedral elements in ANSYS FLUENT. The two zones are later combined during case setup. Since sliding mesh method will be used in this project, therefore there is no need for a conformal mesh at the interface.

Local refinement was done to make the mesh dense in the regions of interest while keeping the total number of cells low. Two bodies of influence, shown in maroon and blue colour in *figure [5]*, were constructed surrounding the propeller blades under this strategy. To capture the boundary layer, inflation layers (see *Appendix A.1*) were grown on the blade surface with first layer thickness of $2x10^{-6}$ m to conform to $y^+<1$ as discussed in the theory section.
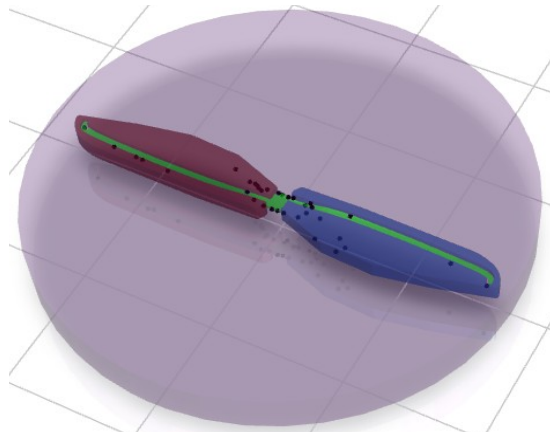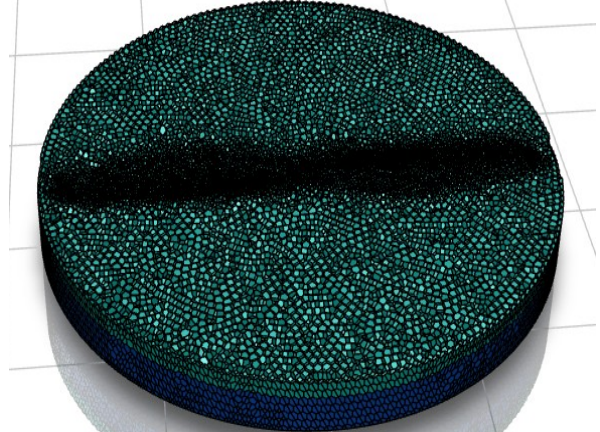

| *Figure 5: Rotor Zone Geometry* | *Figure 6: Polyhedral rotor zone mesh* |

To conduct a mesh convergence study, three different meshes were made by changing the cell sizing parameters. However, the inflation layer parameters were kept same for all meshes. *Table [1]* summarizes the mesh size information used in this research project.

Table 1: Mesh Size Information of Different Models

Model	Number of Cells in Rotor Domain	Number of Cells in Stator Domain	Total Number of Cells in the Model
tsst	3986399	1904000	5890399
tsst1	4339287	2211897	6551184
tsst2	5641047	2707200	8348247

5.3 Model case setup and variation

Three meshes were simulated as described above. The *case-file*[6] was setup for each mesh with same settings. Definition of materials, selection of the appropriate solver equations, boundary conditions, cell zone conditions, solver method, solver controls and other parameters are given in this setup. Air was used as fluid with properties ρ=1.225 *kg/m^3* , μ=1.7894 x 10^{-05} *kg/m-s*.

All the simulations were run in a transient-state condition with a *bounded 2nd-order implicit* temporal discretization. The timestep was set at 10^{-05} *sec* for the first 20 steps to allow the solution to stabilize. The rest of the simulation was carried out with timestep size of 2.7 x 10^{-05} *sec*. The *SIMPLE* algorithm was set for the pressure-velocity coupling. A second order upwind discretization scheme was used for convection terms in pressure and momentum equation while a first order upwind scheme was chosen for all other equations. For cell zone condition, *sliding mesh motion* option with angular velocity of 6000 *RPM* along the *y*-axis was enabled for the rotor zone. The velocity formulation was done in absolute frame for all models as prescribed in the ANSYS theory guide. The convergence criteria was set to 10^{-04} for all the variables. Attention was given during the initialization of the models, since the results depend on the initial condition of the model. The propeller is starting from rest, hence, the pressure and velocity fields are zero everywhere in the interior of the computational domain at the start. As discussed in the theory section, *Transition-SST* model was used to model turbulence for all meshes. After analysing the mesh convergence study, the mesh with optimum performance and accurate result will be selected. Two more models based on this chosen mesh will then be made with different turbulence modelling. (Korfmann 2020) used *kω-SST* for the thesis work, so one model will be tested with this turbulence model and will be named as "kwsst". For the second model, the default *Transition-SST* model will be appended with '*curvature-correction*' option to inspect its influence and will be called "tsstcc". The RSM approach, as mentioned in theory section, is emulated by the '*curvature-correction*' option within *Transition-SST* model. The results for both these models will be compared against default *Transition-SST* turbulence model.

6. Outputs and Discussion

The simulation results were compared against the experimental data provided by the '*Professur für Dynamik und Mechanismentechnik (DMT)*'. The experiments were conducted on a wooden test-bench with a mounted propeller such that the generated thrust is in the direction of gravity. The angular velocity was measured and varied to monitor the changes in sensor values of thrust and moment. 96 Intel[(R)] Xeon[(R)] E5-2680 v3 processor cores with 1.6 Gb of RAM per processor core, were allocated on four compute nodes using MPI architecture on the HPC to all simulation models, in order to contrast them for optimum performance. *Table [2]* summarizes the simulation results and time taken for completion, for all five models. The airflow after 14 rotations visualized in *appendix A.2* verifies the model setup and interfacing between the two zones.

---

[6]*A text or binary file containing mesh data, solver settings and control settings, which is written by ANSYS Fluent after pre-processing steps. This file is used as input to start the simulation. It can also be exported for later use.*

Table 2: Simulation Output and Performance

Model	T_{sim} [N]	%age deviation from T_{exp}	M_{sim} [N-m]	%age deviation from M_{exp}	Time taken to complete [hrs]
kwsst	18.67	-2.4	0.3721	5.8	13.22
tsst	19.1033	-0.14	0.3726	5.94	15.78
tsstcc	18.98	-0.78	0.3690	4.92	15.76
tsst1	19.15	0.1	0.3717	5.69	19.4
tsst2	19.06	-0.37	0.3658	4.01	29.26

The experimental values of thrust and moment are T_{exp} =19.13 N and M_{exp}=0.3517 N-m respectively. The percentage change in thrust values between tsst/tsst1 and tsst1/tsst2 are respectively 0.24% and 0.47%. While the change in time required for simulation between tsst/tsst1 and tsst1/tsst2 are 22.94% and 50.82% respectively. As expected, the computational effort increases significantly with the increase in mesh size. Moreover, refining the mesh produces negligible change in thrust and moment output, suggesting that the output for tsst model is mesh insensitive, in other words mesh is converged. *Figure [7]* shows the mesh convergence study results.
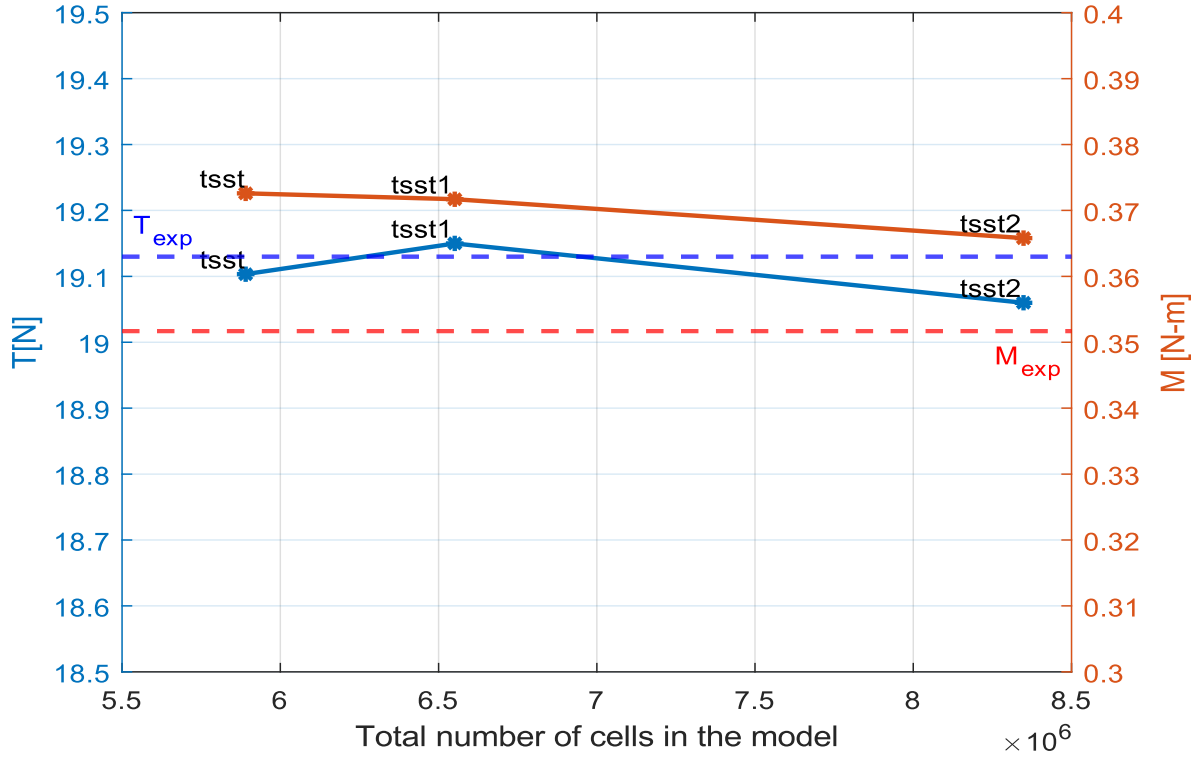

Figure 7: Mesh Convergence Study

Having validated for spatial convergence, it was considered prudent to check for temporal convergence. The timestep size was calculated to accommodate 360 steps per rotation. The corresponding *Courant number* was small. The implicit time discretization scheme used in this project ensures solution convergence regardless of the *Courant number*. However, a large *Courant number* can lead to an inaccurate converged value. To analyse this factor, the timestep size was reduced to 8.35×10^{-06} *sec* and implemented for tsst2 model. It was observed that the time requirement for simulation became three times to that of the original while the output thrust values showed a change of less than 1%. This corroborates to temporal convergence. Hence, the mesh and timestep size used in tsst model was deemed converged and was used in kwsst and tsstcc models for further investigations.

It is quite apparent in *Table [2]*, that tsst gives the best estimation for generated thrust between tsst, kwsst and tsstcc models. The results are in congruence with the theoretical expectation. The *Transition-SST* turbulence model performed better than the *kω-SST* for low *Reynolds-number* flow simulations conducted in this project. The increase in computational time, however, can be explained by the fact that there are two extra equations solved in *Transition-SST* modelling. The '*curvature-correction*' option, explained in the theory section, artificially dampens/bumps-up the calculated turbulence to emulate the effects of vortex and eddies. This is reflected by the dampened value of generated thrust in tsstcc model. Due to its accuracy and efficiency, tsst model turns out to be the most optimum among all the five simulation models tested in this research project. *Figures [8]* and *[9]* respectively shows the thrust and moment curves plotted in time domain.

Figure 8: Instantaneous thrust generated during propeller motion
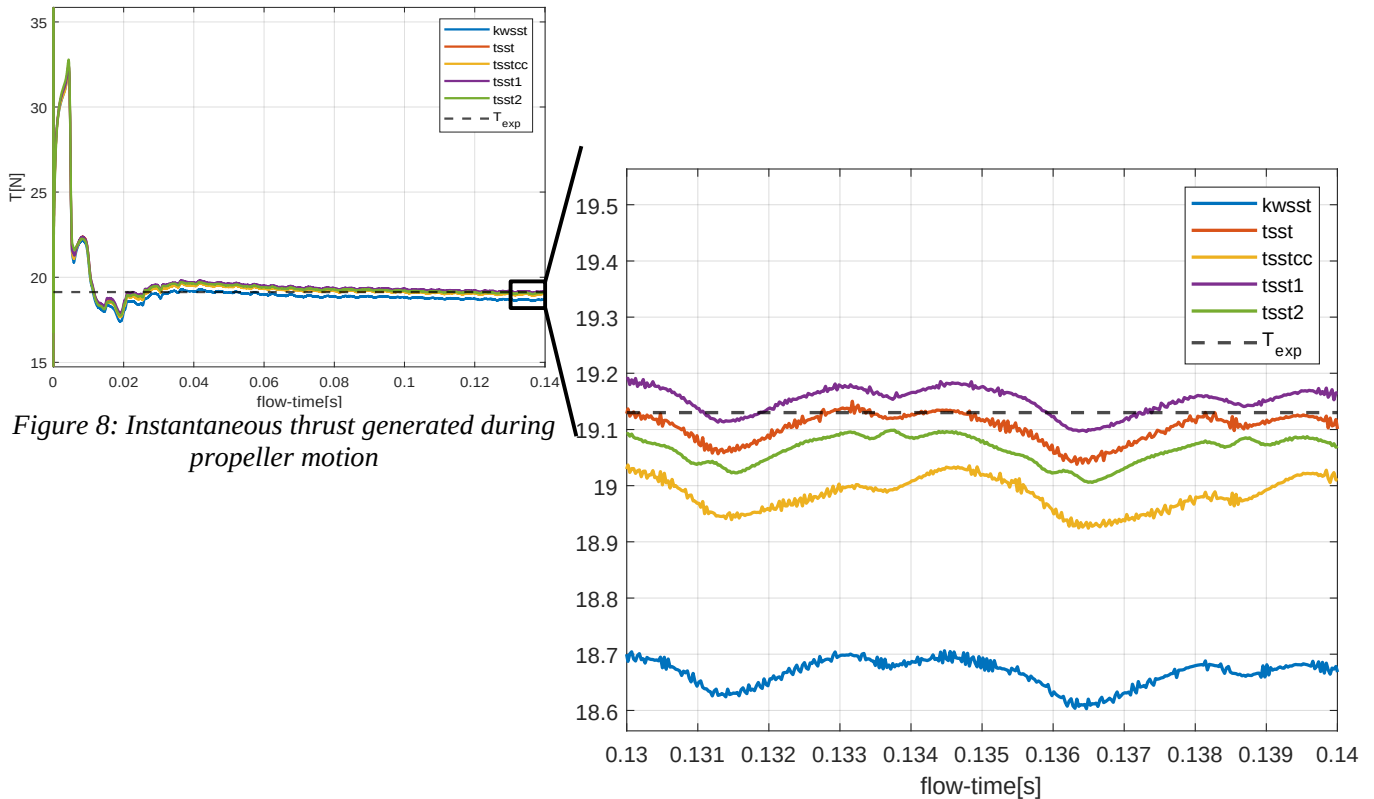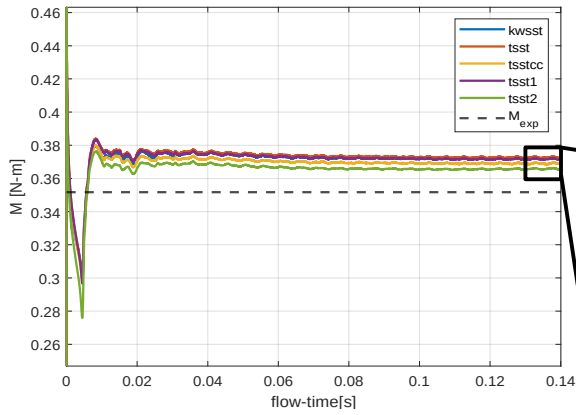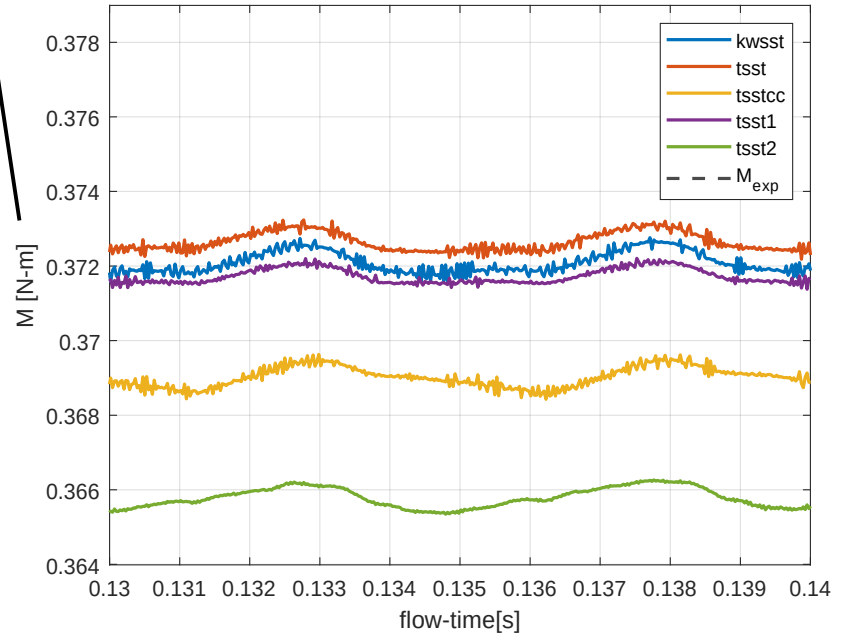
Figure 9: Instantaneous moment during propeller motion

With the aim of conducting vibration analysis, *FFT* transformation was done for the thrust and moment curves of all five models. *Figures [10]* and *[11]* depict the transformed thrust and moment curves respectively. Fulfilling the expectation, the first amplitude appears at 200*Hz*. The propeller is simulated to rotate at a frequency of 100*Hz*. Therefore, any given point in the locus defined by the propeller motion, encounters the propeller blade twice in one rotation. Similarly,
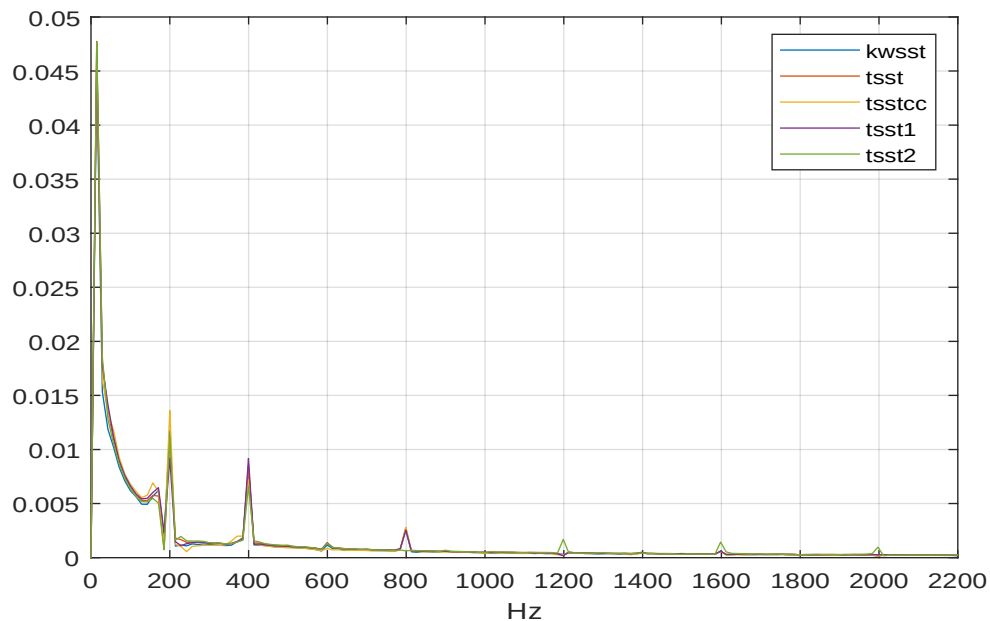

Figure 10: FFT Transformed thrust plot

14

the amplitudes of higher-order vibration waves appear at multiples of 200 on the frequency axis. This trend is qualitatively similar for all five models. Moreover, it is evident that tsst2 model was able to discern more number of wave-orders, which could be a consequence of its high mesh density.
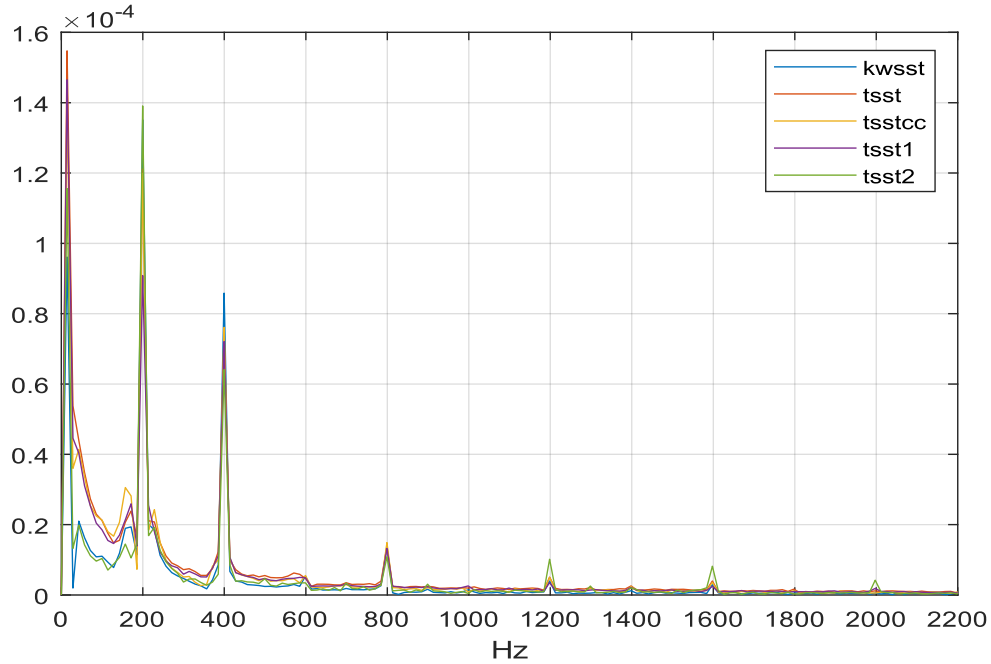

Figure 11: FFT transformed moment plot

7. Conclusion

The problem of vibration phenomena in UAV is being studied in industry and academia. Having the same pursuit in mind, vibration excitation due to aerodynamic turbulence in propeller flows was taken up in this research project. Computational fluid dynamic simulation models were developed for propeller flow. Previous diploma work and ANSYS guides were used to familiarize with modelling techniques for propeller flows.

Experimental data provided by the '*Professur für Dynamik und Mechanismentechnik (DMT)*' served as the benchmark to validate the modelling work. Mesh convergence study was carried out which resulted in three models. The models were studied for spatial and temporal convergence. Further two models were developed, one with a modified *Transition-SST* and other with *kω-SST* to contrast the estimated turbulence. In total five models were developed to optimize the model for vibration analysis purpose. *Transition-SST* turbulence model came out to be the most accurate in estimating the generated thrust, which verifies its purpose to outperform *kω-SST* for low *Reynolds-number* flow problems.

FFT transformation of the generated thrust and moment curves, resulted from the CFD models, agrees with theoretical expectations. The wave frequencies were identified, at which amplitudes of different orders of wave appear. This will help in designing drone parts with natural frequencies different from the ones identified in the *FFT* graphs, to avoid the resonance between

15

aerodynamic vibrations and drone parts. Generally, drone parts are designed with very high natural frequencies, to endure high values of rotor *RPM* during drone flight. These CFD models can be employed to simulate any *RPM* motion and identify the threshold frequency value from the *FFT* graphs to design the drone parts with appropriate characteristics.

References

1. Eric Vargas Loureiro, Nicolas Lima Oliveira, Patricia Habib Hallak, Flávia de Souza Bastos, Lucas Machado Rocha, Rafael Grande Pancini Delmonte, Afonso Celso de Castro Lemonge. Evaluation of low fidelity and CFD methods for the aerodynamic performance of a small propeller. *Aerospace Science and Technology* **108**, 106402 (2021). http://dx.doi.org/https://doi.org/10.1016/j.ast.2020.106402

2. Jon Verbeke, S Debruyne. Vibration analysis of a UAV multirotor frame. (2016).https://www.researchgate.net/publication/313846241_Vibration_analysis_of_a_UAV_multirotor_frame

3. Endrowednes Kuantama, Ovidiu Gheorghe Moldovan, Ioan Ţarcă, Tiberiu Vesselényi, Radu Ţarcă. Analysis of quadcopter propeller vibration based on laser vibrometer. *Journal of Low Frequency Noise, Vibration and Active Control* **40** (2021).https://doi.org/10.1177%2F1461348419866292

4. Masahiko Mizui, Ikuo Yamamoto, Ryouga Ohsawa. Resonance Analysis of the UAV Rotor-arm part. *IOSR Journal of Engineering* **Vol.2**, pp.28-32 (2012). http://dx.doi.org/10.9790/3021-02862832

5. stanisław Radkowski, Przemysław Szulim. Analysis of Vibration of Rotors in Unmanned Aircraft. *Advances in Intelligent Systems and Computing* **317**, 363-371 (2015). http://dx.doi.org/10.1007/978-3-319-10990-9_34

6. Ravindra Krishnamurthy. Meshing Aspects for Open Water Marine Propeller CFD. (2020). https://blog.gridpro.com/meshing-aspects-for-open-water-marine-propeller-cfd/

7. C. Paz, E. Suárez, C. Gil, J. Vence. Assessment of the methodology for the CFD simulation of the flight of a quadcopter UAV. *Journal of Wind Engineering and Industrial Aerodynamics* **218**, 104776 (2021). http://dx.doi.org/https://doi.org/10.1016/j.jweia.2021.104776

8. Weijia Fu, Jie Li, Haojie Wang. Numerical Simulation of Propeller Slipstream Effect on A Propeller-driven Unmanned Aerial Vehicle. *Procedia Engineering* **31**, 150-155 (2012). http://dx.doi.org/https://doi.org/10.1016/j.proeng.2012.01.1005

9. Daniel LaCroix, Radek Máca. Potsdam Propeller CFD Benchmark.https://www.cfdsupport.com/potsdam-propeller-benchmark.html

10. Huilan Yao, Huaixin Zhang. A simple method for estimating transition locations on blade surface of model propellers to be used for calculating viscous force. *International Journal of Naval Architecture and Ocean Engineering* **10** (2017). http://dx.doi.org/10.1016/j.ijnaoe.2017.09.002

11. Sören Korfmann. Simulative Bestimmung charakteristischer Rotorparameter von Multikoptern und Vergleich mit Versuchsergebnissen. (2020).

12. By aokomoriuta（青子守歌） - Own work, CC BY-SA 3.0, https://commons.wikimedia.org/w/index.php?curid=15672321

13. David Wall. Optimum propeller design for electric uavs. (2012). https://etd.auburn.edu/bitstream/handle/10415/3158/David_Wall_Thesis.pdf?sequence=2&ts=1425425356032

14. Y.A. Çengel. Fluid Mechanics. Tata McGraw Hill Education Private, 2010.https://books.google.de/books?id=c8ATbn9ChB8C

15. Jian P. Shao Tuncer Cebeci. Computational Fluid Dynamics for Engineers - From Panel to Navier-Stokes Methods with Computer Programs. Springer Berlin Heidelberg, 2005.

16. Britannica, The Editors of Encyclopaedia. "propeller". Encyclopedia Britannica, 20 Jul. 2012, https://www.britannica.com/technology/propeller .Accessed 23 February 2022.

Appendix

A.1
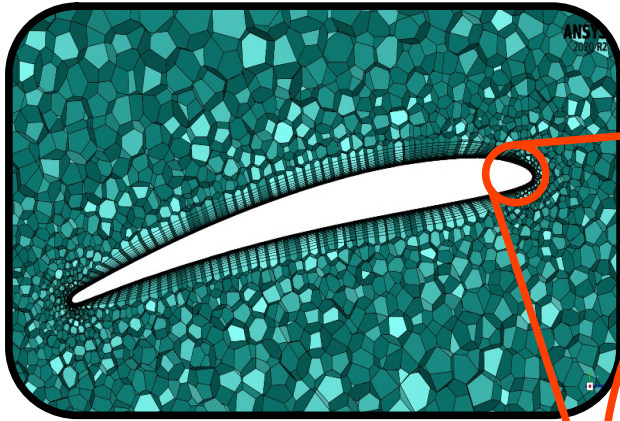
Figure 12: Cross-section view of rotor zone mesh

A.2

2.618e+01

2.291e+01

1.964e+01

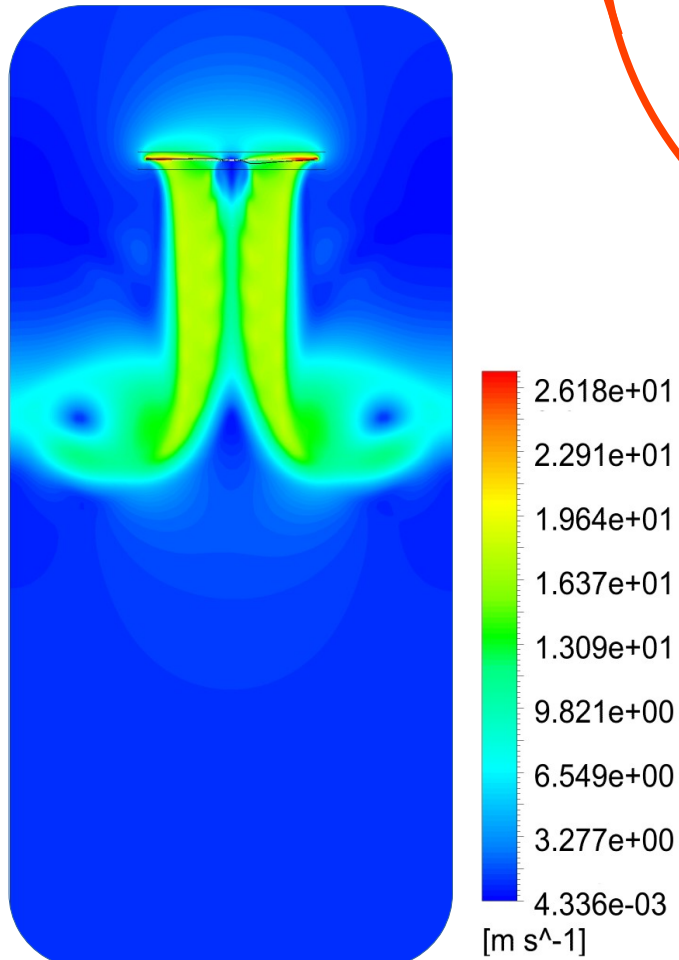1.637e+01

1.309e+01

9.821e+00

6.549e+00

3.277e+00

4.336e-03
[m s^-1]

Figure 13: Velocity contour for y-component of the domain flow